Magnetic Properties of Metal Diphosphonate Compounds with One-Dimensional Chain Structures

Ping Yin,[†] Song Gao,[‡] Li-Min Zheng,*[,†] and Xin-Quan Xin[†]

State Key Laboratory of Coordination Chemistry, Coordination Chemistry Institute, Nanjing University, Nanjing 210093, P. R. China, and State Key Lab of Rare Earth Materials Chemistry and Applications, Peking University, Beijing 100871, P. R. China

Received March 27, 2003. Revised Manuscript Received June 6, 2003

Two new phosphonate compounds $(NH_4)_2M_2(hedpH)_2$ (M = Co, **1**; Fe, **2**), where hedp is 1-hydroxyethylidenediphosphonate [$CH_3C(OH)(PO_3)_2$], have been synthesized under hydrothermal conditions at 140 °C. Crystal data: **1**, triclinic, $P\bar{1}$, a = 5.4635(13) Å, b = 7.7205(18) Å, c = 9.976(2) Å, α = 71.198(4)°, β = 82.385(4)°, γ = 87.920(5)°, V = 394.82(16) Å^3, Z = 1; **2**, triclinic, P1, a = 5.5191(12) Å, b = 7.7183(16) Å, c = 10.051(2) Å, α = 71.551(4)°, β = 82.552(4)°, γ = 87.627(4)°, V = 402.74(15) Å^3, Z = 1. The compounds are isomorphous; all contain anionic double chains of $\{M_2(hedpH)_2\}_n^{2n-}$, composed of $\{MO_6\}$ octahedra and $\{CPO_3\}$ tetrahedra. The double chain can be viewed as a ladder within which dimers of $\{M_2(\mu-O)_2\}$ (rung) are separated by O−P−O bridges (rail). Very strong hydrogen bonds exist between the neighboring chains, hence forming a layer in the *ab* plane. The NH_4^+ counterions occupy the cavities within the layer. These layers are further connected by hydrogen bonds to form a three-dimensional network. The temperature-dependent magnetic susceptibility measurements show dominant antiferromagnetic interactions in both compounds, mediated through the μ−O and/or O−P−O bridges between the metal centers. The field dependent magnetization reveals that both experience field-induced magnetic transitions at very low temperatures. The critical fields at 1.9 K are ca. 35 kOe for **1** and 40 kOe for **2**, respectively.

Introduction

A major interest in metal phosphonate chemistry in recent years has been the syntheses of compounds with new structure types, especially porous structures, because of their potential applications in exchange, catalysis, and sensors.[1−5] Research studies on the metal phosphonate compounds as molecule-based magnetic materials are not well documented. However, some interesting magnetic behaviors have been observed in such systems. For example, weak ferromagnetic or canted antiferromagnetic behavior was observed in some Mn(II), Fe(II), and Co(II) compounds including $Mn(C_nH_{2n+1}PO_3)\cdot H_2O$,[6] $Fe(RPO_3)\cdot H_2O$ (R = C_2H_5, C_6H_5),[7,8] $Co_3(O_3PC_2H_4CO_2)_2$,[9] and $\{K_2[CoO_3PCH_2N(CH_2CO_2)_2]\}_6\cdot xH_2O$.[10] In a few layered Cu−hedp compounds [hedp = 1-hydroxyethylidenediphosphonate, $CH_3C(OH)(PO_3)_2$], metamagnetism was found.[11] To discover new magnetic materials based on metal phosphonates, herein we report the syntheses, crystal structures, and magnetic properties of two new M−hedp compounds with one-dimensional ladder-like chain structures, namely $(NH_4)_2Co_2(hedpH)_2$ (**1**) and $(NH_4)_2Fe_2(hedpH)_2$ (**2**).

It is worth noting that one-dimensional magnetic materials, especially the quantum spin systems with a finite energy gap above the singlet ground state, have been the current focus of much interest.[12−15] Such quantum spin systems include even-leg spin ladders and ferromagnetic−antiferromagnetic alternating chains. When the applied magnetic field reaches a critical point, the energy gap in these systems is closed, hence a 3D magnetic ordering can be observed. The magnetic measurements on compounds **1** and **2** reveal that both show dominant antiferromagnetic interactions, and they

* To whom correspondence should be addressed. Fax: +86-25-3314502 or 3317761. E-mail: lmzheng@netra.nju.edu.cn.
[†] Nanjing University.
[‡] Peking University.

(1) Clearfield, A. In *New Developments in Ion Exchange Materials*; Abe, M., Kataoka, T., Suzuki, T., Eds.; Kodansha, Ltd.: Tokyo, 1991.
(2) Cao, G.; Hong, H.-G.; Mallouk, T. E. *Acc. Chem. Res.* **1992**, 25, 420.
(3) Alberti, G. *Comprehensive Supramolecular Chemistry*; Lehn, J. M., Ed.; Pergamon/Elsevier Science, Ltd.: Oxford, U. K., 1996; vol. 7.
(4) Clearfield, A. In *Progress in Inorganic Chemistry, Vol. 47*; Karlin, K. D., Ed.; John Wiley & Sons: New York, 1998; pp 371−510.
(5) Vermeulen, L. A. In *Progress in Inorganic Chemistry, Vol. 44, Molecular Level Artificial Photosynthetic Materials*; Meyer, G. J., Ed.; John Wiley & Sons: New York, 1997; p 143.
(6) Carling, S. G.; Visser, D.; Kremer, R. K. *J. Solid State Chem.* **1993**, *106*, 111.
(7) Bujoli, B.; Pena, O.; Palvadeau, P.; Le Bideau, J.; Payen, C.; Rouxel, J. *Chem. Mater.* **1993**, *5*, 583.
(8) Bellitto, C.; Federici, F.; Altomare, A.; Rizzi, R.; Ibrahim, S. A. *Inorg. Chem.* **2000**, *39*, 1803.
(9) Rabu, P.; Janvier, P.; Bujoli, B. *J. Mater. Chem.* **1999**, *9*, 1323.
(10) Gutschke, S. O. H.; Price, D. J.; Powell, A. K.; Wood, P. T. *Angew. Chem., Int. Ed.* **1999**, *38*, 1088.
(11) (a) Yin, P.; Zheng, L.-M.; Gao, S.; Xin, X.-Q. *Chem. Commun.* **2001**, 2346; (b) Zheng, L.-M.; Gao, S.; Song, H.-H.; Decurtins, S.; Jacobson, A.-J.; Xin, X.-Q. *Chem. Mater.* **2002**, *14*, 3143.
(12) Sachdev, S. *Science* **2000**, *288*, 475.
(13) Tandon, K.; Lal, S.; Pati, S. K.; Ramasesha, S.; Sen, D. *Phys. Rev. B* **1999**, *59*, 396.
(14) Carlin, R. L. *Magnetochemistry*; Springer-Verlag: Berlin/Heidelberg, 1986.
(15) Watson, B. C.; Kotov, V. N.; Meisel, M. W.; Hall, D. W.; Granroth, G. E.; Montfrooij, W. T.; Nagler, S. E.; Jensen, D. A.; Backov, R.; Petruska, M. A.; Fanucci, G. E.; Talham, D. R. *Phys. Rev. Lett.* **2001**, *86*, 5168. Landee, C. P.; Turnbull, M. M.; Galeriu, C.; Giantsidis, J.; Woodward, F. M. *Phys. Rev. B* **2001**, *63*, 100402. Oosawa, A.; Katori, H. A.; Tanaka, H. *Phys. Rev. B* **2001**, *63*, 134416. Azuma, M.; Hiroi, Z.; Takano, M.; Ishida, K.; Kitaoka, Y. *Phys. Rev. Lett.* **1994**, *73*, 3463. Eccleston, R. S.; Barnes, T.; Brody, J.; Johnson, J. W. *Phys. Rev. Lett.* **1994**, *73*, 2626.

10.1021/cm034206l CCC: $25.00
Published on Web 07/11/2003

experience field-induced phase transitions at low temperature, suggesting a quasi quantum spin behavior.

Experimental Section

Materials and Methods. All the starting materials were reagent grade and used as purchased. The 50% aqueous solution of 1-hydroxyethylidenediphosphonic acid ($hedpH_4$) was purchased from Nanjing Shuguang Chemical Factory of China. The elemental analyses were performed on a PE 240C elemental analyzer. The infrared spectra were recorded on a Nicolet 170SX FT-IR spectrometer with pressed KBr pellets. The magnetic susceptibility measurements for **1** and **2** were carried out on polycrystalline samples (41.8 mg for **1**, 29.8 mg for **2**) using a MagLab System 2000 magnetometer in a magnetic field up to 7 T. Diamagnetic corrections were estimated from Pascal's constants.[16]

Synthesis of $(NH_4)_2Co_2(hedpH)_2$, 1. A mixture of $CoCl_2 \cdot 6H_2O$ (1 mmol, 0.2393 g), 50% $hedpH_4$ (1 cm^3), and H_2O (8 cm^3), adjusted by $NH_3 \cdot H_2O$ to pH 3.33, was kept in a Teflon-lined autoclave at 140 °C for 2 d. After slow cooling to room temperature, purple-red needlelike crystals were collected as a monophasic material, judged by the powder X-ray diffraction pattern, which were further used for the structural determination and the physical properties measurements. Yield: 37% based on Co. Anal. found: 9.01; H, 3.67; N, 5.58. Calcd for $C_4H_{18}Co_2N_2O_{14}P_4$: C, 8.57; H, 3.21; N, 5.00. IR (KBr, cm^{-1}): 3413s, 3168s, 3052s, 2936s, 2873s, 1704w, 1680w, 1478m, 1463m, 1440m, 1400m, 1378w, 1331w, 1267m, 1125s, 1042s, 999m, 914s, 884s, 803m, 669m, 585m, 549m, 491w, 456m, 417w. The addition of pyrazine (1 mmol), which may serve as a template, to the above reaction mixture resulted in the same product with an increased yield (50% based on Co). The same compound can also be produced when the amount of $CoCl_2$ was increased to 1.5 mmol and/or the pH of the mixture varied between 3 and 4. A lower pH (∼2) promotes the formation of an unidentified purple powder.

Synthesis of $(NH_4)_2Fe_2(hedpH)_2$, 2. A mixture of $FeSO_4 \cdot 7H_2O$ (1 mmol, 0.2784 g), 50% $hedpH_4$ (1 cm^3), and H_2O (8 cm^3), adjusted by $NH_3 \cdot H_2O$ to pH 3.07, was treated hydrothermally at 140 °C for 2 d. Pale yellow needlelike crystals were produced as a single phase, judged by the powder X-ray pattern in comparison with the pattern deduced from single-crystal data. Yield: 33% based on Fe. Anal. found: C, 8.96; H, 3.62; N, 5.04%. Calcd for $C_4H_{18}Fe_2N_2O_{14}P_4$: C, 8.67; H, 3.25; N, 5.06%. IR (KBr, cm^{-1}): 3417s, 3156s, 3049s, 2938s, 2871s, 1682w, 1479m, 1441m, 1406m, 1376w, 1333w, 1268m, 1146s, 1124s, 1078s, 1040s, 998m, 918s, 886m, 802m, 668m, 583m, 547m, 487m, 456m, 409m. The compound **2** can be obtained similarly when the pH is increased to 4. The addition of pyrazine (1 mmol) to the above reaction mixture resulted in the same product with an increased yield (47% based on Fe). A lower pH (∼2) or a higher ratio of Fe/50%$hedpH_4$ (1.5−2.0 mmol:1.0 cm^3) led to the formation of an unidentified light green powder. The light green powder was also observed when a prolonged reaction time (72 h) was employed for the above-mentioned reaction.

X-ray Crystallographic Analysis. Crystals with dimensions 0.10 × 0.02 × 0.02 mm for **1** and 0.15 × 0.02 × 0.02 mm for **2** were selected for indexing and intensity data collection at 293(2) K on a Bruker SMART APEX CCD diffractometer with monochromated Mo Kα (λ = 0.71073 Å) radiation. A hemisphere of data was collected using a narrow-frame method with scan widths of 0.30° in ω and an exposure time of 20 s/frame for **1** and 10 s/frame for **2**. The data were integrated using the Siemens SAINT program,[17] with the intensities corrected for Lorentz factor, polarization, air absorption, and absorption due to variation in the path length through the detector faceplate. Empirical absorption was applied for both compounds.

Table 1. Crystallographic Data

compound	**1**	**2**
formula	$C_4H_{18}N_2Co_2O_{14}P_4$	$C_4H_{18}N_2Fe_2O_{14}P_4$
M_r	559.94	553.78
crystal system	triclinic	triclinic
space group	$P\bar{1}$	$P\bar{1}$
a/Å	5.4635(13)	5.5191(12)
b/Å	7.7205(18)	7.7183(16)
c/Å	9.976(2)	10.051(2)
α/°	71.198(4)	71.551(4)
β/°	82.385(4)	82.552(4)
γ/°	87.920(5)	87.627(4)
V/Å^3	394.82(16)	402.74(15)
Z	1	1
D_c/g cm^{-3}	2.355	2.283
F(000)	282	280
μ(Mo Kα)/cm^{-1}	25.86	22.77
goodness of fit on F^2	0.908	1.024
R1, wR2[a] [$I>2\sigma(I)$]	0.0353, 0.0662	0.0398, 0.1009
(all data)	0.0459, 0.0688	0.0439, 0.1033
$(\Delta\rho)_{max}$, $(\Delta\rho)_{min}$/e Å^{-3}	0.454, −0.585	0.839, −0.680

[a] $R_1 = \Sigma||F_o| - |F_c||/\Sigma|F_o|$. $wR_2 = [\Sigma w(F_o^2 - F_c^2)^2/\Sigma w(F_o^2)^2]^{1/2}$.

Table 2. Selected Bond Lengths [Å] and Angles [°] for 1[a]

Co(1)−O(5A)	2.023(2)	Co(1)−O(4B)	2.059(2)
Co(1)−O(2A)	2.091(2)	Co(1)−O(1)	2.119(2)
Co(1)−O(4)	2.160(2)	Co(1)−O(7)	2.252(2)
P(1)−O(2)	1.505(2)	P(1)−O(1)	1.512(2)
P(1)−O(3)	1.580(3)	P(1)−C(2)	1.840(3)
P(2)−O(6)	1.509(2)	P(2)−O(5)	1.511(2)
P(2)−O(4)	1.539(2)	P(2)−C(2)	1.845(4)
O(5A)−Co(1)−O(4B)	99.31(10)	O(5A)−Co(1)−O(2A)	88.00(9)
O(4B)−Co(1)−O(2A)	103.64(9)	O(5A)−Co(1)−O(1)	169.22(9)
O(4B)−Co(1)−O(1)	91.46(9)	O(2A)−Co(1)−O(1)	89.98(9)
O(5A)−Co(1)−O(4)	95.10(9)	O(4B)−Co(1)−O(4)	79.84(9)
O(2A)−Co(1)−O(4)	174.93(10)	O(1)−Co(1)−O(4)	86.23(9)
O(5A)−Co(1)−O(7)	90.92(9)	O(4B)−Co(1)−O(7)	157.64(9)
O(2A)−Co(1)−O(7)	96.49(9)	O(1)−Co(1)−O(7)	78.79(9)
O(4)−Co(1)−O(7)	79.48(8)	P(1)−O(1)−Co(1)	117.53(13)
P(1)−O(2)−Co(1C)	135.86(15)	P(2)−O(4)−Co(1B)	137.41(13)
P(2)−O(4)−Co(1)	117.57(13)	Co(1B)−O(4)−Co(1)	100.16(9)
P(2)−O(5)−Co(1C)	140.57(15)	C(2)−O(7)−Co(1)	104.84(18)

[a] Symmetry transformations used to generate equivalent atoms: A $x-1, y, z$; B $-x+1, -y+1, -z+1$; C $x+1, y, z$.

The structures were solved by direct methods and refined on F^2 by full-matrix least squares using SHELXTL.[18] All the non-hydrogen atoms were refined anisotropically. All the hydrogen atoms were assigned fixed isotropic thermal parameters 1.4 or 1.5 times the equivalent isotropic U of the atoms to which they are attached, and were refined isotropically. Selected crystallographic data and structure determination parameters are given in Table 1, and selected bond lengths and angles are provided in Tables 2 and 3 for **1** and **2**, respectively.

Results and Discussion

Crystal Structures. Compounds **1** and **2** are isomorphous. Each crystallizes in space group $P\bar{1}$, and contains $\{M_2(hedpH)_2\}_n^{2n-}$ double chains and NH_4^+ counterions. Figure 1 shows a fragment of the double chain in structure **1** with atomic labeling scheme. The cobalt atom has a strongly distorted octahedral environment with the O−Co−O bond angles ranging from 78.79(9) to 174.93(10)°. The Co−O bond lengths fall between 2.023(2) and 2.252(2) Å. The $hedpH^{3-}$ ligand, singly protonated at O(3), chelates and bridges the Co(II) ions into an infinite single chain by using four of its phosphonate oxygens [O(1), O(2), O(4), and O(5)] and the hydroxyl oxygen [O(7)]. The remaining phosphonate oxygen, O(6), remains pendant [P(2)−O(6) 1.509(2) Å].

(16) Kahn, O. *Molecular Magnetism*; VCH Publishers: New York, 1993.

(17) *SAINT*, Program for Data Extraction and Reduction, Siemens Analytical X-ray Instruments Inc.: Madison, WI, 1994−1996.

(18) Sheldrick, G. M. *SHELXTL PC*, version 5; Siemens Analytical X-ray Instruments Inc.: Madison, WI, 1995.

Table 3. Selected Bond Lengths [Å] and Angles [°] for 2[a]

Fe(1)−O(5A)	2.043(2)	Fe(1)−O(4B)	2.094(2)
Fe(1)−O(2A)	2.128(2)	Fe(1)−O(1)	2.137(2)
Fe(1)−O(4)	2.197(2)	Fe(1)−O(7)	2.325(2)
P(1)−O(2)	1.506(2)	P(1)−O(1)	1.520(2)
P(1)−O(3)	1.576(2)	P(1)−C(2)	1.843(3)
P(2)−O(6)	1.509(2)	P(2)−O(5)	1.511(2)
P(2)−O(4)	1.541(2)	P(2)−C(2)	1.849(3)
O(5A)−Fe(1)−O(4B)	101.17(9)	O(5A)−Fe(1)−O(2A)	87.17(9)
O(4B)−Fe(1)−O(2A)	105.73(9)	O(5A)−Fe(1)−O(1)	167.41(9)
O(4B)−Fe(1)−O(1)	91.40(9)	O(2A)−Fe(1)−O(1)	90.14(9)
O(5A)−Fe(1)−O(4)	96.18(9)	O(4B)−Fe(1)−O(4)	78.37(9)
O(2A)−Fe(1)−O(4)	174.16(8)	O(1)−Fe(1)−O(4)	85.56(9)
O(5A)−Fe(1)−O(7)	90.55(9)	O(4B)−Fe(1)−O(7)	154.79(9)
O(2A)−Fe(1)−O(7)	96.98(9)	O(1)−Fe(1)−O(7)	77.56(8)
O(4)−Fe(1)−O(7)	78.24(8)	P(1)−O(1)−Fe(1)	118.19(12)
P(1)−O(2)−Fe(1C)	136.16(14)	P(2)−O(4)−Fe(1B)	135.93(14)
P(2)−O(4)−Fe(1)	117.86(12)	Fe(1B)−O(4)−Fe(1)	101.63(9)
P(2)−O(5)−Fe(1C)	140.64(14)	C(2)−O(7)−Fe(1)	104.38(18)

[a] Symmetry transformations used to generate equivalent atoms: A $x-1, y, z$; B $-x+1, -y+1, -z+1$; C $x+1, y, z$.

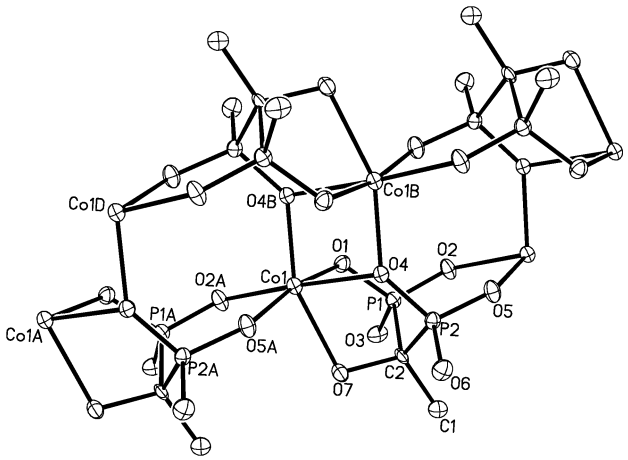

Figure 1. Chain fragment with atomic labeling scheme (50% probability) in **1**.

The two single chains are cross linked by the O(4) atoms, forming a ladder with the edge sharing $\{Co_2(\mu-O)_2\}$ dimers as the rung. An inversion center lies in the middle of the shared edge. The Co(1)−O(4)−Co(1B) angle is 100.16(9)°. The Co···Co distance over the μ−O(4) bridge is 3.236 Å, and those across the O−P−O bridges are 5.463 and 4.754 Å for Co(1)···Co(1A) and Co(1)···Co(1D), respectively.

Between the adjacent chains, there exist very strong hydrogen bonds between the protonated oxygen O(3) and the pendant O(6) [O(3)···O(6) 2.544 Å], thus forming a layer in the *ab* plane (Figure 2). The NH_4^+ cations occupy the intralayer cavities, and are stabilized by hydrogen bonds toward the phosphonate oxygens [O(1), O(2), O(5), and O(6)] of the $\{Co_2(hedpH)_2\}_n$ chains. The shortest interchain Co···Co distance is 7.010 Å within the layer. The layers are connected by the hydrogen bond contacts through the hydroxyl O(7) atom from one layer and the phosphonate O(3) atom from the other [O(7)···O(3) 2.882 Å], hence generating a three-dimensional network (Figure 3).

The structure of **2** is analogous to that of **1** except that the Fe(II) ions replace the Co(II) ions. Consequently, the Fe−O bond lengths in **2** range from 2.043(2) to 2.325(2) Å. Within the double chains, the Fe···Fe distance over the μ−O(4) bridge and the Fe(1)−O(4)−Fe(1B) angle are 3.327 Å and 101.6(1)°, respectively. The Fe···Fe distances across the O−P−O bridges are 5.519 for

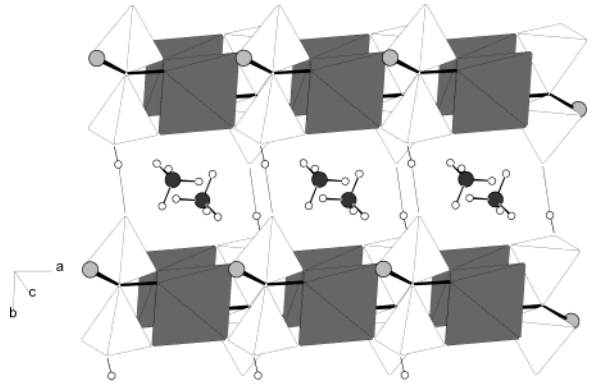

Figure 2. One layer of structure **1** in the *ab* plane showing the hydrogen bonding interactions between the double chain and the NH_4^+ cations.

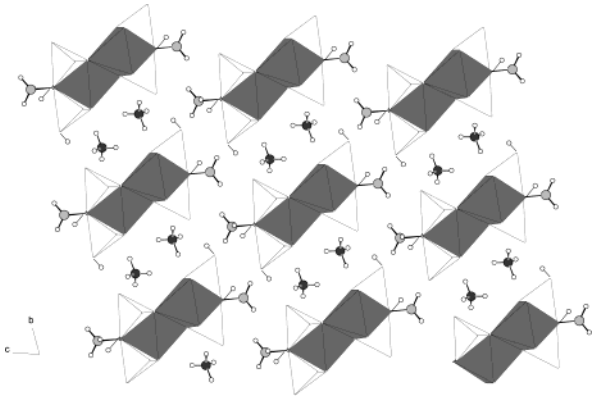

Figure 3. Polyhedral representation of the structure of **1** viewed along the *a*-axis.

Fe(1)···Fe(1A) and 4.712 Å for Fe(1)···Fe(1D), respectively.

Compound **2** can be compared to the related compounds $[NH_3(CH_2)_nNH_3]Fe_2(hedpH)_2\cdot 2H_2O$ ($n = 4, 5$)[19] where the diprotonated 1,4-diaminobutane and 1,5-diaminopentane were the charge compensating counterions. Although all three contain similar $\{Fe_2(hedpH)_2\}_n$ double chains, they differ significantly in the packing of their structures. In the latter cases, each double chain is linked to its four equivalent neighbors through very strong hydrogen bonds, thus forming a three-dimensional open network with channels where the $[NH_3(CH_2)_nNH_3]^{2+}$ cations and lattice water reside. In compound **2**, however, each $\{Fe_2(hedpH)_2\}_n$ double chain has six nearest neighbors of the equivalent chain, connected by strong or moderate hydrogen bonds.

Magnetic Properties. Figure 4 shows the molar magnetic susceptibilities (χ_M), measured at 10 kOe for **1**, as a function of temperature. The observed magnetic moment per Co atom is 5.28 μ_B at 300 K, much higher than the spin only values expected for high spin Co(II) (3.87 μ_B), attributing to the orbital contribution of the cobalt ion. On cooling from 300 K, a rounded peak appears at about 11 K, typical for low-dimensional antiferromagnetic compounds.[14] The weak antiferromagnetic exchange is also confirmed by a negative Weiss constant (−34.1 K) determined by the data in the temperature range 100−300 K. The *ac* susceptibility

(19) Zheng, L.-M.; Song, H.-H.; Lin, C.-H.; Wang, S.-L.; Hu, Z.; Yu, Z.; Xin, X.-Q. *Inorg. Chem*. **1999**, *38*, 4618. Song, H.-H.; Zheng, L.-M.; Zhu, G.; Shi, Z.; Feng, S.; Gao, S.; Xin, X.-Q. *Chin. J. Inorg. Chem*. **2002**, *18* (1), 67.

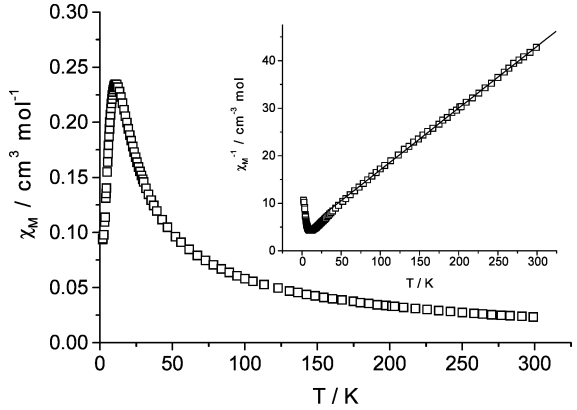

Figure 4. Plots of χ_M and $^1/\chi_M$ vs T for **1**.

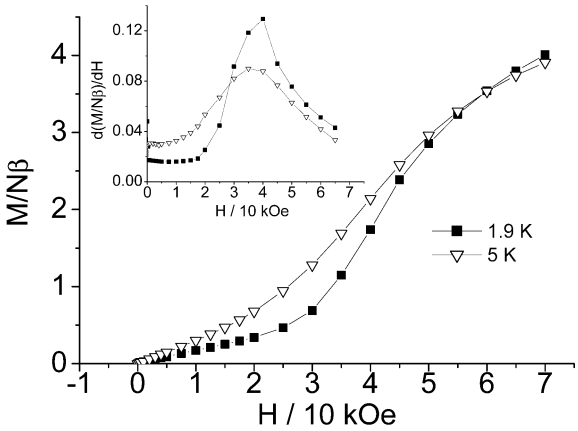

Figure 5. Field dependent magnetization of **1** at 1.9 and 5 K.

measurements performed in the range 5−20 K, at H_{ac} = 5 Oe and frequencies of 111, 199, 355, 633, and 1111 Hz, show neither an out-of-phase signal nor frequency-dependent behavior (Figure S1 in the Supporting Information). The broad maximum around 10 K is consistent with a low-dimensional antiferromagnetic material (Figure S1). Considering that the structure of **1** contains $\{Co_2(hedpH)_2\}_n$ chains linked by interchain hydrogen bonds, the interchain magnetic exchanges through the O−P−O−H···O−P−O bridges are appreciably weak. The dominant antiferromagnetic interaction could be propagated within the ladder-like chain through μ−O and/or O−P−O bridges. Therefore, the system can be viewed as a quasi one-dimensional antiferromagnet. A sharp drop of χ_M toward zero at very low temperature suggests that the ground state of the system is $S = 0$ (Figure 4). Figure 5 shows the field dependence of magnetizations of **1** at 1.9 and 5.0 K. The clear sigmoid shape of the curve indicates the occurrence of a magnetic transition from the antiferromagnetic ground state to a spin polarized state. The transition field, determined by dM/dH derivative curve, is ca. 35−40 kOe depending on the temperature. For the Co(II) ion in an octahedral environment, an $S = {}^1/_2$ ground state is usually observed at low temperatures because of the overall effect of crystal field and spin−orbit coupling. The magnetization of **1** at 70 kOe is 4.0 Nβ per Co_2 unit, close to the saturation value of 4.1 Nβ anticipated for a pair of $S = {}^1/_2$ spins with $g = 4.1$.[20]

For compound **2**, both the *dc* (measured at 10 kOe) and *ac* (measured at H_{ac} = 5 Oe) magnetic susceptibilities are consistent with a low-dimensional antiferromagnet, with the rounded peaks appearing at ca. 20 K (Figure 6 and Figure S2). The magnetization with a typical sigmoid shape is also observed at 1.9 and 5.5 K (Figure 7). The transition field is ca. 40−45 kOe depending on the measuring temperature. The magnetization of **2** at 70 kOe is 5.8 Nβ per Fe_2 unit, less than the saturation value of 8 Nβ anticipated for two independent $S = 2$ spin with $g = 2.0$.

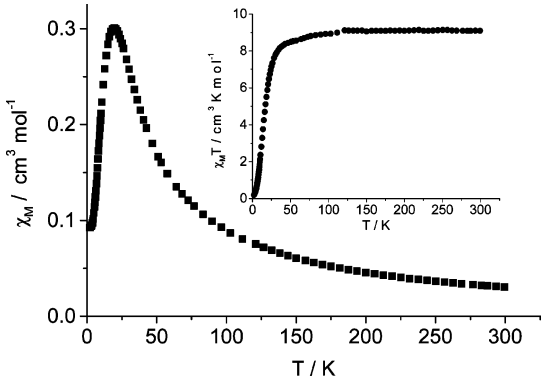

Figure 6. Plots of χ_M and $\chi_M T$ vs T for **2**.

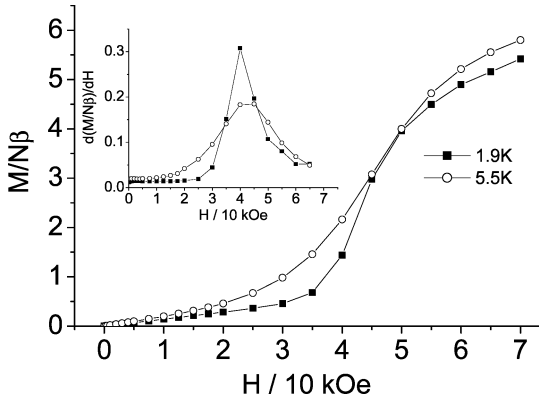

Figure 7. Field dependent magnetization of **2** at 1.9 and 5.5 K.

In summary, this paper describes the syntheses and crystal structures of two isomorphous phosphonate compounds: $(NH_4)_2Co_2(hedpH)_2$ (**1**) and $(NH_4)_2Fe_2(hedpH)_2$ (**2**). They exhibit a one-dimensional ladder-like chain structure with extensive hydrogen bonding interactions between the chains. The magnetic properties of both compounds show dominant antiferromagnetic interactions between the magnetic centers. The field-induced magnetic transitions are observed, with the critical fields at 1.9 K at ca. 35 kOe for **1** and 40 kOe for **2**, respectively. The result indicates that both compounds may be viewed as quasi one-dimensional quantum spin systems.

Acknowledgment. We thank the National Natural Science Foundation of China, the Ministry of Education of China, and the Natural Science Foundation of Jiangsu province of China for financial support, and Mr. Yong-Jiang Liu for crystal data collection.

Supporting Information Available: Crystallographic data for **1** and **2** (CIF). This material is available free of charge via the Internet at http://pubs.acs.org.

CM034206L

(20) Caneschi, A.; Dei, A.; Gatteschi, D.; Tangoulis, V. *Inorg. Chem.* **2002**, *41*, 3508.